

# Fine Mapping of the 1p36 Deletion Syndrome Identifies Mutation of *PRDM16* as a Cause of Cardiomyopathy

Anne-Karin Arndt,<sup>1,2</sup> Sebastian Schafer,<sup>3</sup> Jorg-Detlef Drenckhahn,<sup>3</sup> M. Khaled Sabeh,<sup>2</sup> Eva R. Plovie,<sup>2</sup> Almuth Caliebe,<sup>4</sup> Eva Klopocki,<sup>5,6</sup> Gabriel Musso,<sup>2</sup> Andreas A. Werdich,<sup>2</sup> Hermann Kalwa,<sup>2</sup> Matthias Heinig,<sup>3,7</sup> Robert F. Padera,<sup>8</sup> Katharina Wassilew,<sup>9</sup> Julia Bluhm,<sup>10</sup> Christine Harnack,<sup>10</sup> Janine Martitz,<sup>10</sup> Paul J. Barton,<sup>11,12</sup> Matthias Greutmann,<sup>13</sup> Felix Berger,<sup>14,15</sup> Norbert Hubner,<sup>3,16</sup> Reiner Siebert,<sup>4</sup> Hans-Heiner Kramer,<sup>1</sup> Stuart A. Cook,<sup>11,17,18</sup> Calum A. MacRae,<sup>2,19</sup> and Sabine Klaassen<sup>10,15,19,\*</sup>

Deletion 1p36 syndrome is recognized as the most common terminal deletion syndrome. Here, we describe the loss of a gene within the deletion that is responsible for the cardiomyopathy associated with monosomy 1p36, and we confirm its role in nonsyndromic left ventricular noncompaction cardiomyopathy (LVNC) and dilated cardiomyopathy (DCM). With our own data and publicly available data from array comparative genomic hybridization (aCGH), we identified a minimal deletion for the cardiomyopathy associated with 1p36del syndrome that included only the terminal 14 exons of the transcription factor *PRDM16* (PR domain containing 16), a gene that had previously been shown to direct brown fat determination and differentiation. Resequencing of *PRDM16* in a cohort of 75 nonsyndromic individuals with LVNC detected three mutations, including one truncation mutant, one frameshift null mutation, and a single missense mutant. In addition, in a series of cardiac biopsies from 131 individuals with DCM, we found 5 individuals with 4 previously unreported nonsynonymous variants in the coding region of *PRDM16*. None of the *PRDM16* mutations identified were observed in more than 6,400 controls. *PRDM16* has not previously been associated with cardiac disease but is localized in the nuclei of cardiomyocytes throughout murine and human development and in the adult heart. Modeling of *PRDM16* haploinsufficiency and a human truncation mutant in zebrafish resulted in both contractile dysfunction and partial uncoupling of cardiomyocytes and also revealed evidence of impaired cardiomyocyte proliferative capacity. In conclusion, mutation of *PRDM16* causes the cardiomyopathy in 1p36 deletion syndrome as well as a proportion of nonsyndromic LVNC and DCM.

## Introduction

Chromosome 1p36 deletion syndrome (MIM 607872) is the most common human terminal deletion syndrome, occurring in 1 out of 5,000 births.<sup>1</sup> Among the major characteristics of the syndrome are craniofacial dysmorphism, structural brain abnormalities, seizure disorder, hearing loss, intellectual disability, and growth delay.<sup>2–4</sup> A substantial proportion (23%–27%) of individuals with 1p36 deletion syndrome have cardiomyopathy, which may occur in the presence or absence of structural heart disease.<sup>3,4</sup> In a systematic clinical and molecular characterization of a 1p36 deletion syndrome cohort, left ventricular noncompaction (LVNC [MIM 604169]) was identified in 23% and dilated cardiomyopathy (DCM [MIM 115200]) in 4% of in-

dividuals.<sup>4</sup> LVNC is a common feature in early embryopathy in humans and in rodent models and is characterized by a two-layered myocardium consisting of a thin compacted epicardial layer and a thick noncompact endocardial layer with numerous prominent ventricular trabeculations and deep intertrabecular recesses.<sup>5</sup> It can be associated with increased ventricular chamber dimensions and impaired systolic function, which are cardinal features of DCM. Both LVNC and DCM are genetically heterogeneous, with mutations in genes encoding sarcomeric, cytoskeletal, mitochondrial, and calcium handling proteins causing either phenotype.<sup>6</sup> Clinical features of both cardiomyopathies include progressive deterioration in cardiac function that results in heart failure, arrhythmias, and sudden cardiac death. Loss or disruption of a gene

<sup>1</sup>Department of Congenital Heart Disease and Pediatric Cardiology, University Hospital of Schleswig-Holstein, Campus Kiel, 24105 Kiel, Germany;

<sup>2</sup>Cardiovascular Division, Brigham and Women's Hospital, Harvard Medical School, and Harvard Stem Cell Institute, Boston, MA 02115, USA; <sup>3</sup>Max-Delbrück-Center for Molecular Medicine (MDC), 13125 Berlin, Germany; <sup>4</sup>Institute of Human Genetics, Christian-Albrechts-University Kiel & University Hospital Schleswig-Holstein, Campus Kiel, 24105 Kiel, Germany; <sup>5</sup>Institute of Medical Genetics and Human Genetics, Charité University Medicine Berlin, 13353 Berlin, Germany; <sup>6</sup>Institute of Human Genetics, University Würzburg, 97074 Würzburg, Germany; <sup>7</sup>Department of Computational Biology, Max Planck Institute for Molecular Genetics, 14195 Berlin, Germany; <sup>8</sup>Department of Pathology, Brigham and Women's Hospital, Harvard Medical School, Boston, MA 02115, USA; <sup>9</sup>Department of Pathology, German Heart Institute Berlin, 13353 Berlin, Germany; <sup>10</sup>Experimental and Clinical Research Center (ECRC), Charité Medical Faculty and Max-Delbrück-Center for Molecular Medicine, 13125 Berlin, Germany; <sup>11</sup>National Heart and Lung Institute, Imperial College, London SW7 2AZ, UK; <sup>12</sup>NIHR Royal Brompton Cardiovascular Biomedical Research Unit, London SW3 6NP, UK; <sup>13</sup>Cardiovascular Center, University Hospital Zürich, 8001 Zürich, Switzerland; <sup>14</sup>Department of Congenital Heart Defects & Pediatric Cardiology, German Heart Institute Berlin, 13353 Berlin, Germany; <sup>15</sup>Department of Pediatric Cardiology, Charité University Medicine Berlin, 13353 Berlin, Germany; <sup>16</sup>DZHK (German Centre for Cardiovascular Research), Partner Site Berlin, Germany; <sup>17</sup>National Heart Centre, Singapore 168752, Singapore; <sup>18</sup>Duke-NUS Graduate Medical School, Singapore 169857, Singapore

<sup>19</sup>These authors contributed equally to this work

\*Correspondence: [klaassen@mdc-berlin.de](mailto:klaassen@mdc-berlin.de)

<http://dx.doi.org/10.1016/j.ajhg.2013.05.015>. ©2013 by The American Society of Human Genetics. All rights reserved.

responsible for the cardiomyopathy in individuals with monosomy 1p36 has not previously been identified.

We present detailed multiallelic mapping in the 1p36 deletion syndrome that identifies loss of *PRDM16* (MIM 605557) as underlying the cardiomyopathy in this syndrome. We independently confirm a causal role for *PRDM16* in human myocardial disease in two separate cohorts: one with nonsyndromic LVNC and one with simplex cases of dilated cardiomyopathy (DCM). We are able to recapitulate biological features of human cardiomyopathy in the zebrafish by modeling of both *PRDM16* haploinsufficiency and a human truncation mutant. This modeling implicates impaired proliferative capacity during cardiogenesis as a primary mechanism of these inherited forms of heart failure caused by *PRDM16* mutations.

## Material and Methods

### Comparative Genomic Hybridization

Genomic imbalances were analyzed by array comparative genomic hybridization (aCGH) with different oligonucleotide platforms (Agilent Technologies) at the Charité University Hospital Berlin<sup>7</sup> and University Hospital Schleswig-Holstein, Kiel.<sup>8</sup> Further genomic and phenotypic data from probands with monosomy 1p36 (Tables S1 and S2 available online) were extracted from the following databases: Decipher,<sup>9</sup> ECARUCA database,<sup>10</sup> NCBI, and Genoglyphix. Genomic positions in the text are cited according to the reference human genome (UCSC Genome Browser GRCh37/hg19) (Table S1).

### Study Participants and Clinical Evaluation

A total of 206 probands with nonsyndromic cardiomyopathy were recruited at tertiary referral centers, the Charité University Hospital and the German Heart Institute (both in Berlin, Germany), the University Hospital Zürich (Switzerland), and the Harefield Hospital (Harefield, UK). Informed consent was obtained from all participants according to institutional guidelines. Probands and available family members were clinically evaluated as described previously.<sup>11</sup> LVNC and DCM were diagnosed on the basis of established criteria.<sup>5,12</sup> A total of 75 individuals with LVNC were studied and only LVNC probands without a known mutation in genes encoding sarcomere proteins were enrolled in the study. In 56/75 probands, no mutations had been detected and 19/75 probands had not been tested.<sup>13</sup> In 11/75 LVNC probands, at least one more first-degree relative had been clinically diagnosed to be affected but not all first-degree family members were systematically available and could be investigated. For RNA-seq studies, 131 explanted heart biopsies samples from individuals with confirmed DCM undergoing heart transplantation were used with local ethical approval. From probands with DCM, the family history and the number of familial or simplex cases was unknown and they had not been screened for mutations in genes encoding sarcomere proteins.

### Mutational Analysis

PCR and Sanger sequencing of *PRDM16* (RefSeq accession number NM\_022114.3) in probands with LVNC or DCM and of *SKI* (MIM 164780 [RefSeq NM\_003036.3]) in probands with LVNC were performed by standard methods. Primer sequences and

PCR details are available on request. Sequences were analyzed with Sequencher 4.10.1 (Gene Codes Corporation). In the 131 DCM individuals, poly(A) RNA was sequenced on the Illumina HiSeq 2000 platform with TruSeq library preparation and 2 × 100 bp paired-end sequencing chemistry. Reads were mapped stringently against the hg19 reference genome with Tophat 1.3.1,<sup>14</sup> allowing only a total of 2 mismatches in 100 bp and supplying transcript information as annotated by the Ensembl database<sup>15</sup> to aid the mapping process. SNP calling in the coding region of *PRDM16* was performed with SAMtools<sup>16</sup> only with reads mapping uniquely to the genome. Genomic positions covered with more than 15 unique reads (no PCR duplicates) were considered for SNP detection.

### Immunofluorescence Staining and Microscopy

Paraffin sections of 19-week-old fetal and adult human left ventricular myocardium (48-year-old male individual as donor for heart transplantation; cause of death was subarachnoid hemorrhage) and wild-type embryonic mouse hearts (13.5 dpc) were deparaffinized and rehydrated and heat-mediated antigen retrieval was performed in sodium citrate buffer (10 mM [pH 6.0]) for 20 min. Sections were allowed to cool to room temperature before blocking in antibody solution containing 5% normal goat serum for 1 hr. For staining of adult mouse hearts, cryosections of fresh frozen cardiac tissue were used after 20 min postfixation in 4% PFA. Primary antibodies were applied at 4°C overnight, sections were washed three times in PBS, and secondary antibody detection was performed at room temperature for 1 hr with Alexa 488 or Alexa 555 goat anti-rabbit or goat anti-mouse antibodies (Invitrogen). Nuclei were stained with TO-PRO-3 or DAPI (Invitrogen) and sections were mounted in Prolong Gold antifade reagent (Invitrogen). The primary antibodies used were rabbit anti-*PRDM16* (Abcam) and mouse anti-Troponin T (Developmental Studies Hybridoma Bank at the University of Iowa). For staining cell membranes, FITC-conjugated wheat germ agglutinin (WGA) was used while endocardial cells were stained with FITC-conjugated Isolectin B4 (Enzo Life Sciences), both of which were incubated together with the primary antibody at 4°C overnight. The specificity of *PRDM16* staining was tested by preincubating the primary *PRDM16* antibody with the respective immunizing peptide (Acris Antibodies) at 4°C overnight prior to the immunofluorescence procedure. Images were taken with a Leica SP5 confocal laser-scanning microscope.

### Zebrafish Studies

#### Morpholino Antisense Oligonucleotide Injections

Antisense morpholinos were injected as described<sup>17</sup> at the one-cell stage. Concentrations of 0.2 mM were used; for synergistic experiments the concentration was reduced to 0.1 mM. Embryos were then analyzed at 24, 48, and 72 hr postfertilization (hpf). Morpholinos directed against the translation start codon were 5'-TCATCGCTGTCTCCCGCTCCTGCT-3' for *prdm16*, 5'-TAATC GATGCTTACCACTCCTCCT-3' for *prdm16* mismatch control, and the splice donor site of exon 2 5'-TCGCTCTCC TCCCCATCGTTTCCCT-3' for *skia* (RefSeq NM\_130935.2). Morpholinos were purchased from Gene Tools.

#### Cardiac Overexpression

For cardiac-specific overexpression experiments, the human *PRDM16* truncation mutation (c.2104A>T [p.Lys702\*]) and the human *PRDM16* wild-type were cloned downstream of the *cmlc2* promoter into the Tol2kit expression system by Gateway

technology (Invitrogen). We coinjected the *PRDM16* constructs (15 ng/ $\mu$ l) with 10 ng/ $\mu$ l capped Tol2 transposase mRNA into one-cell-stage zebrafish embryos.

#### Rescue Experiments

To rescue the cardiac phenotype, different doses of human wild-type mRNA were coinjected with either *PRDM16* morpholino or *PRDM16* truncation construct into the one-cell-stage zebrafish embryo.

#### Zebrafish Physiologic Analysis

For analysis of cardiac function, embryos were laterally positioned and allowed to acclimate at 24°C. Video microscopy was performed on an Axioplan (Zeiss) upright microscope with a Fast-Cam-PCI high-Speed digital camera (Photron) on top. A total of 1,088 frames were digitally captured at identical frame rates (250 frames per second) and magnification (5 $\times$ ). Sequential images were analyzed for heart rate and cardiac output by IMAGEJ and Excel. Experiments were repeated at least three times on each occasion with ten animals.

Intercellular coupling parameters in zebrafish embryo hearts were measured by previously reported techniques.<sup>18</sup> In brief, hearts were isolated from zebrafish embryos, stained with the transmembrane-potential-sensitive dye di-8-ANEPPS (Invitrogen), and placed into a perfusion chamber that was mounted onto the stage of an inverted microscope. Excitation light from a high-intensity Hg arc lamp was transmitted through a 525/50 nm band-pass filter and reflected onto the preparation via a 565 nm dichroic mirror. Fluorescence emission was filtered by a 685/80 nm band-pass filter and recorded at a rate of 2,000 s<sup>-1</sup> by a high-speed CCD camera (CardioCCD-SMQ, RedshirtImaging, LLC). Single-pixel action potentials were extracted from the fluorescence data and conduction velocities were estimated by an established algorithm. Experiments were repeated at least two times with five animals.

#### RNA In Situ Hybridization, Immunofluorescence, and Detection of Apoptosis

24-, 48-, and 72-hpf-old zebrafish embryos were used for in situ hybridization carried out by standard protocols with fluorescein-labeled sense and antisense RNA probes for *prdm16* (RefSeq XM\_01922892.3).

For proliferation detection, hearts from 28-, 48-, 72-, and 96-hpf-old zebrafish embryos were isolated and fixed in Prefer fixative (Anatech). The fixed hearts were stained with the primary antibodies rabbit anti-PCNA 1:200 (Abcam) and mouse anti-MF20 1:100 (DSHB) and with the secondary antibodies donkey or goat anti-rabbit or mouse Alexa 488 or 546 conjugated (Invitrogen) 1:1,000. Hearts were mounted with ProLong Antifade reagent with DAPI mounting medium on a slide. Confocal images were analyzed with IMAGEJ.

For detection of apoptosis, hearts from 48-, 72-, and 96-hpf-old zebrafish embryos were isolated and fixed in 4% PFA/PBS for 30 min and washed twice in PBS-T for 30 min. TUNEL assay was performed with the in situ cell detection kit from Roche. Hearts were mounted with ProLong Antifade reagent with DAPI on a slide and confocal images were analyzed with IMAGEJ. Transgenic *cmlc-Gal4* zebrafish embryos were either coinjected with *PRDM16* truncation construct or *PRDM16* morpholino and UAS-Annexin-V-YFP construct or alone with the UAS-Annexin-V-YFP construct<sup>19</sup> (a gift from Dr. Randall T. Peterson) at the one cell stage. 48-, 72-, and 96-hpf-old zebrafish hearts were isolated and fixed in 4% PFA/PBS for 20 min and washed twice in PBS-T for 30 min. Then the hearts were mounted with ProLong Antifade reagent with DAPI on a slide. Confocal images were analyzed with

IMAGEJ. A minimum of five animals were used for each time point.

#### Statistical Analysis

For functional experiments in zebrafish, one-way ANOVA was used. Fisher's exact test was used to test the significance of mutational variants found in nonsyndromic LVNC and DCM. Data are presented as means  $\pm$  SEM.  $p < 0.05$  was considered statistically significant for all tests; \* $p < 0.05$ , \*\* $p < 0.005$ , \*\*\* $p < 0.0005$ .

## Results

### Alignment of Regions of Loss in Individuals with 1p36 Deletion Syndrome and Cardiomyopathy

In order to identify potential candidate genes involved in the pathogenesis of the cardiac phenotypes in chromosome 1p36 deletion syndrome, we aligned the regions of chromosomal loss in individuals with cardiomyopathy from our institutional cohorts and from publicly available databases (Figure 1A). In total, we identified 18 individuals (17 from available databases and 1 from our institution) with a deletion in 1p36 with evidence of heart muscle disease (Figure 1A and Table S1). Various extracardiac phenotypes were present in the 18 individuals with cardiomyopathy, most frequently developmental delay (13/18) and intellectual disability (11/18) (Table S2). With the exception of a single case that had a very large deleted segment (7.2 Mb), all identified individuals shared a minimal region of loss at chr1: 3,224,674–3,354,772 bp (UCSC Genome Browser GRCh37/hg19) that affected only a single gene, *PRDM16*. In particular, exons 4–17 of *PRDM16* were included in the minimal interval, suggesting perturbation of the function of this gene as the cause of the cardiomyopathy in chromosome 1p36 deletion syndrome.

### Identification of *PRDM16* Point Mutations in Nonsyndromic Cardiomyopathy

To independently assess the role of *PRDM16* mutations as a genetic cause of cardiomyopathy, we extended our analyses to nonsyndromic forms of both LVNC and DCM. We sequenced the entire coding region of *PRDM16* in 75 unrelated individuals of Western European descent (49 men and 26 women; mean age, 43 years; range 0.4 to 78 years) that had previously been diagnosed with LVNC via standard criteria. Heterozygous *PRDM16* mutations were identified in 3/75 probands that were not present in 156 in-house control subjects or in the 1000 Genomes Project ( $p = 0.00021$ ) (Figures 1B, 2, and S1A). The LVNC mutations all resided in the large exon 9 of *PRDM16* and included one truncation (c.2104A>T [p.Lys702\*]), one frameshift null mutation (c.1573dupC [p.Arg525Profs\*79]), and one missense mutation (c.2447A>G [p.Asn816Ser]) affecting an amino acid residue with complete evolutionary conservation to zebrafish. Figure 2 describes the phenotype of three LVNC probands with *PRDM16* mutations. To evaluate DCM subjects, we performed RNA-seq on RNA extracted from 131 heart biopsies

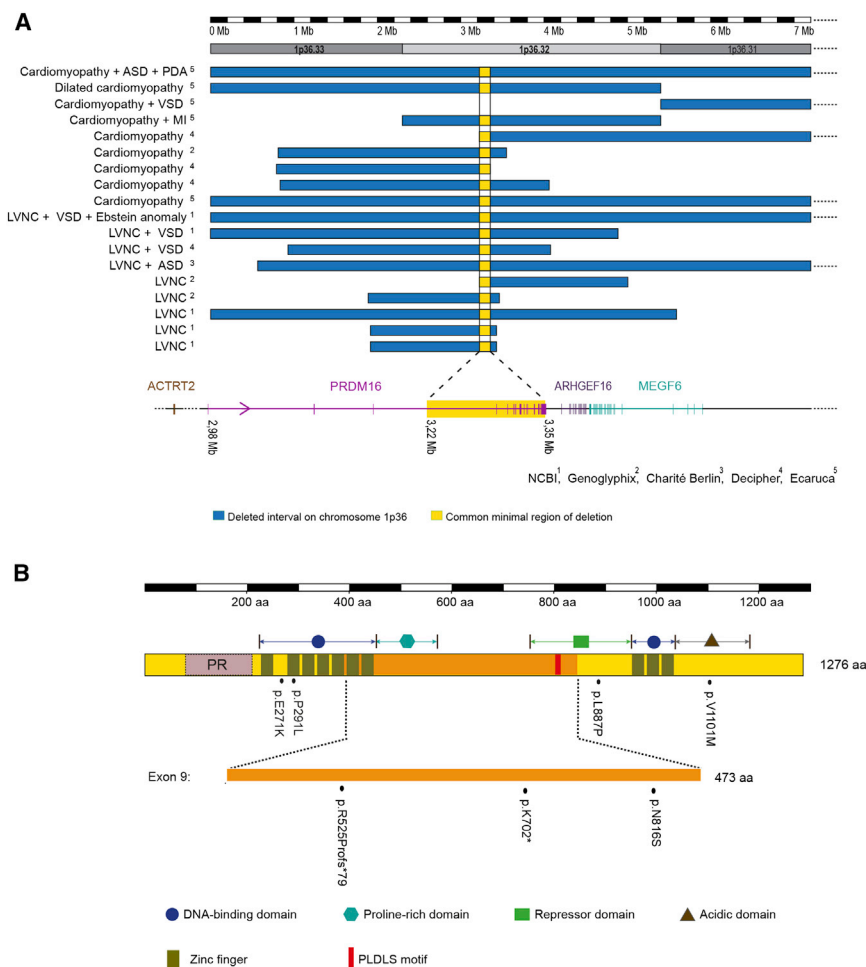


**Figure 1. Alignment of Regions of Loss in Individuals with 1p36del Syndrome Associated with Cardiomyopathy and Identification of *PRDM16* Mutations in Nonsyndromic LVNC and DCM**

(A) Mapping in 18 probands (for further information see Tables S1 and S2) with chromosome 1p36 deletion syndrome and cardiomyopathy shows the respective 1p36-deleted intervals (blue, according to the five data sources: NCBI, Genoglyphix, Charite Berlin, Decipher, and Ecaruca) and the common minimal region of deletion (yellow) to contain the *PRDM16* gene (GRCh37/hg19). The common minimal region (yellow) in probands with cardiomyopathy comprises of 130,098 bp at 3,224,674–3,354,772 bp in 17/18 probands and contains exon 4–17 of *PRDM16*. Abbreviations are as follows: ASD, atrial septal defect; VSD, ventricular septal defect; PDA, patent ductus arteriosus; MI, mitral insufficiency.

(B) *PRDM16* domain structure with conserved motifs and binding domains and location of amino acid changes in three nonsyndromic LVNC and five nonsyndromic DCM probands. The three mutations in LVNC are all located in exon 9 (orange); two DCM probands share the same substitution (p.Val1101Met). The complete *PRDM16* 1,276 aa containing protein with the N-terminal PR domain (violet), two zinc finger DNA binding domains (black bars), and a PLDLS motif at position 804–808 (red bar) is shown. The PR region corresponds to a SET domain, an 130 amino acid, evolutionarily conserved sequence motif with histone

methyltransferase activity. The ten zinc finger domains correspond to the classical C2H2-type, in which the first pair of zinc-coordinating residues are cysteines and the second pair are histidines, conferring zinc-dependent DNA- or RNA-binding properties.

obtained from unrelated individuals with simplex cases of the disorder. This identified four previously unreported nonsynonymous variants in the coding region of *PRDM16* in five individuals. These variants were confirmed by Sanger sequencing of genomic DNA from peripheral blood (Figures 1B and S1B). The four identified variants were not listed by the 1000 Genomes Project or detected in the more than 6,400 control individuals of the Exome Sequencing Project (ESP) and were thus considered novel. Considering the prevalence of missense variants in *PRDM16* ( $n = 55$  in 6,400 exomes) in the ESP control population, we would expect only ~1.2 novel mutations in a set of 131 individuals. When compared to the novel variants identified from the 6,400 individuals sequenced by ESP, this represents a more than 4-fold enrichment of novel nonsynonymous coding variants ( $p = 0.006$ ). The significant enrichment of novel nonsynonymous variants affecting *PRDM16* in the cohort further supports a role for *PRDM16* in DCM. One mutation is located in a zinc finger domain of exon 6 (c.872C>T [p.Pro291Leu]) and three individuals are affected by mutations that disrupt the coding sequence at the C terminus of *PRDM16* that mediates the regulation of TGF $\beta$  signaling (c.2660T>C [p.Leu887Pro]),

of which two share the same mutation (c.3301G>A [p.Val1101Met]) (Table 1). Only the mutation c.811G>A (p.Glu271Lys) is not linked to any known functional domain. All five missense mutations in probands with LVNC and DCM occur at evolutionarily conserved residues (Figure S1B).

### Cardiac Localization Profile of *PRDM16*

To investigate a potential role for alterations in *PRDM16* in cardiac structure and function, we first evaluated *PRDM16* protein localization in the left ventricle of wild-type mice and in the human heart (Figures 3 and S2). In fetal and adult human heart, *PRDM16* was localized in the nuclei of both cardiomyocytes and interstitial cells. At mouse embryonic day 13.5, *PRDM16* was localized throughout the ventricular myocardium including endocardium and epicardium. In the adult mouse, *PRDM16* localization was predominantly restricted to the nuclei of cardiomyocytes. Taken together, these data support the hypothesis that *PRDM16* is expressed in embryonic and adult mammalian left ventricular myocardium. RNA in situ hybridization in zebrafish revealed predominant expression of *prdm16* in the brain and heart (Figure S3).

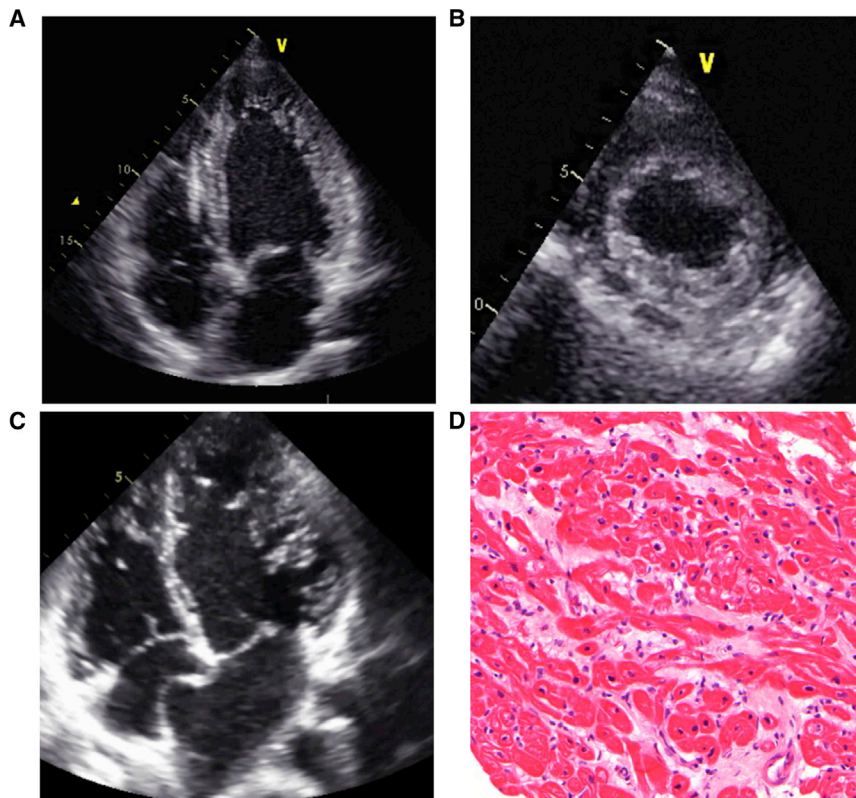


**Figure 2. Left Ventricular Morphology and Clinical Description of LVNC Proband with *PRDM16* Mutations**

(A) Echocardiographic apical 4-chamber view of proband 1 showing involvement of apical and lateral segments. Proband 1 carried a frameshift mutation (c.1573dupC [p.Arg525Profs\*79]) and presented at age 33 years with severe biventricular heart failure with systolic and diastolic dysfunction, secondary pulmonary hypertension, and dilatation of both atria and ventricles. He received a biventricular intracardiac defibrillator.

(B) Short axis view of the same proband at the level below the LV papillary muscles showing marked thickening of the inferior noncompacted layer and thinning of the compacted layer.

(C) Echocardiographic apical 4-chamber view of proband 2 showing involvement of the LV midventricular lateral wall. Proband 2, with a truncation mutation (c.2104A>T [p.Lys702\*]), was diagnosed at age 12 years because of arrhythmias and showed mild to moderate left ventricular dysfunction and dilatation in addition to LVNC.

(D) Haematoxylin staining of LV myocardium of proband 3. In proband 3 a missense mutation (c.2447A>G [p.Asn816Ser]) was detected. He had been sent to cardiac surgery for the

reconstruction of a dysplastic mitral valve at the age of 11 years because of mitral insufficiency grade 3. The left atrium and left ventricle were enlarged with preserved cardiac function. Histology of a left ventricular biopsy taken at cardiac surgery showed increased interstitial fibrosis and myocyte disarray.

### Loss of Function and Mutant Transgenic Analysis in Zebrafish

To examine the effect of *PRDM16* mutations, we performed knockdown of the zebrafish ortholog of *PRDM16* by using translation-blocking morpholinos to recapitulate potential haploinsufficiency. We also generated fish transgenic for the truncated mutant form of *PRDM16* (c.2104A>T [p.Lys702\*]) driven by the cardiac-specific *cmlc2* promoter. Dose-dependent bradycardia was observed and cardiac output was significantly reduced in both morphant ( $p < 0.0005$ ) and in truncation mutant transgenics ( $p < 0.0005$ ) when compared with controls (Figure 4A). Importantly, the contractile impairment in both the morphant knockdown embryos and in the truncation mutant transgenics was efficiently rescued by the wild-type human *PRDM16* (Figure S4) in a dose-dependent manner. Notably, to rescue the truncation mutant (Figure S4B), a 10-fold excess of wild-type RNA was necessary compared to the morphant knockdown (Figure S4A).

Semiautomated cell counting documented a significant decrease in total cardiomyocyte numbers in *PRDM16* morphant hearts when compared to WT controls ( $p < 0.05$ ) and *PRDM16* WT ( $p < 0.05$ ) at 48 hpf (Figures 4B and 4C). At 96 hpf, total cardiomyocyte numbers were also decreased in the mutant hearts compared to WT controls ( $p < 0.005$ ) and *PRDM16* WT ( $p < 0.05$ ) (Figure 4C). This was associated with significantly decreased cardiomyocyte proliferation

(percentage of PCNA-positive cells) in the hearts of the morphant ( $p < 0.0005$ ), the truncation ( $p < 0.0005$ ), and *PRDM16*-overexpressing wild-type ( $p < 0.005$ ) hearts at 28 and 48 hpf ( $p < 0.0005$ ;  $p < 0.005$ ;  $p < 0.005$ ) consecutively (Figures 4B and 4C). Proliferation of control WT decreased over time (28–96 hpf). Interestingly, the effects of mutant and wild-type *PRDM16* constructs on proliferation appear to act in opposing directions between 48 or 96 hpf and 72 hpf. In addition, there was evidence of a concomitant increase in apoptosis in the *PRDM16* mutants at 48 hpf by using either TUNEL assay ( $p < 0.005$ ) or annexin V transgenic reporter lines ( $p < 0.005$ ) (Figure S5).

Proliferation is often reciprocally related to cell coupling. In murine models where LVNC is observed, it has been associated with evidence of partial cellular uncoupling, so we tested the effects of *PRDM16* on intercellular impulse propagation across the myocardium, identifying a significant reduction in coupling in morphant and in mutant hearts (Figure 5A). Mean estimated conduction velocities from the outer curvature of the ventricle (OC) confirm a significant reduction in impulse propagation velocities in morphant ( $p < 0.0005$ ) and mutant ( $p < 0.0005$ ) hearts when compared with uninjected controls or wild-type (Figure 5B).

### Genetic Interaction of *PRDM16* with *SKI*

The deletion of the TGF- $\beta$  repressor *SKI* in individuals with 1p36del syndrome has been hypothesized to contribute to

**Table 1. PRDM16 Mutations in Nonsyndromic Proband with LVNC and DCM**

Disease	Variant	Nucleotide Change	Exon	SIFT <sup>a</sup>	PolyPhen-2 <sup>b</sup>	Sequence Features (Uniprot)	Affected Individuals
DCM	p.Glu271Lys	c.811G>A	6	0.16	0.56	–	1
DCM	p.Pro291Leu	c.872C>T	6	0.01	0.75	zinc finger 23 C2H2-type 2	1
LVNC	p.Arg525Profs*79	c.1573dupC	9	–	–	–	1
LVNC	p.Lys702*	c.2104A>T	9	–	–	–	1
LVNC	p.Asn816Ser	c.2447A>G	9	0.23	0.196	–	1
DCM	p.Leu887Pro	c.2660T>C	10	0.00	0.79	mediates interaction with SKI and regulation of TGF-β signaling	1
DCM	p.Val1101Met	c.3301G>A	15	0.15	0.46	mediates interaction with SKI and regulation of TGF-β signaling	2

Abbreviations are as follows: LVNC, left ventricular noncompaction; DCM, dilated cardiomyopathy.

<sup>a</sup>Scores less than 0.05 indicate substitutions are predicted as intolerant.

<sup>b</sup>Scores are evaluated as 0.000 (most probably benign) to 0.999 (most probably damaging).

some of the associated syndromic features.<sup>20</sup> Indeed, in 14 of 18 probands with a deletion in chromosome 1p36, *SKI* was deleted in addition to *PRDM16* (Table S1). To evaluate this possibility, we screened our independent nonsyndromic LVNC cohort for mutations in *SKI*, but no mutations were identified. In addition, we tested for genetic interactions between *PRDM16* and the zebrafish ortholog of *SKI*. Coinjection of subthreshold doses of *PRDM16* and *SKI* MOs reduced cardiac output (Figure 5C), suggesting significant functional synergy between these two genes in their effects on contractility ( $p < 0.0005$ ).

## Discussion

By using existing genomic data, we identified *PRDM16* in the region of minimal genomic overlap in individuals with 1p36 deletion syndrome and cardiomyopathy. We went on to identify mutations in *PRDM16* in two cohorts of nonsyndromic LVNC and DCM, independently confirming a causal role for the gene in these forms of human myocardial disease. Together these data implicate another pathway in the spectrum of known monogenic causes of heart failure and offer the potential for studies of the mechanisms of this morbid condition and possible therapies.

The 1p36del syndrome is the most common form of large-scale terminal deletion observed in humans.<sup>1</sup> Clearly, the disruption or dose reduction of multiple different genes may contribute to the various phenotypes observed in this syndrome and to the pleiotropic manifestations reported.<sup>2–4</sup> We focused on the most specific cardiac phenotype present in the individuals with 1p36del syndrome and were able to identify a minimal interval containing only part of a single gene (*PRDM16*). Several other studies have mapped critical regions within the 1p36 deletion syndrome.<sup>21,22</sup> Candidate genes for features of 1p36del syndrome, including facial clefting anomalies (*SKI*),<sup>20</sup> seizures (*KCNAB2* [MIM 601142]),<sup>23</sup> and cranial suture closure (*MMP23 A/B* [MIM 603320 and 603321]),<sup>24</sup> have been proposed. Gajecka et al.<sup>25</sup> suggested five candidate genes,

among them *PRDM16*, that might contribute to the phenotypic feature of LVNC. *PRDM16* was anticipated to play a role in heart development because mutant mice had gross cardiac ventricular hypoplasia.<sup>26</sup>

Mutations in *SKI* have recently been shown to cause Shprintzen-Goldberg syndrome (MIM 182212) with aortic aneurysm and a role for *SKI* in early cardiovascular development has been proposed.<sup>27,28</sup> Our observation that loss of function of both *SKI* and *PRDM16* act synergistically would support the interaction with *SKI* as a potential mechanism in some of the known deletions. In 14 of our 18 probands with a deletion in chromosome 1p36, *SKI* was deleted in addition to *PRDM16*. Although there were no obvious phenotypic differences between probands with or without a deletion of *SKI*, our studies raise the possibility of a modifier effect of *SKI* in the 1p36del syndrome.

All but one (case 16, arr CGH 1p36(5,400,000–12,700,000)×1) (Table S1) of the individuals with 1p36del syndrome were hemizygous for *PRDM16*. Though knockdown of *PRDM16* and the single *PRDM16* truncation mutant appear equivalent in our zebrafish model, it is certainly possible that perturbation or dose reduction of other genes and/or a long-range regulatory effect<sup>29</sup> within the interval contribute to the cardiac phenotypes observed. Monosomy 1p36 may not be a simple contiguous gene deletion syndrome and deletions of variable size may account for the characteristic phenotype by position effect on one or more genes along the 1p36 region.<sup>30</sup> Several hypotheses have been formed, following the description of different chromosomal rearrangements occurring next to variants in genes that cause human developmental disorders.<sup>31</sup> In case 16, it is unknown whether a position effect would be possible because the distal deletion breakpoint is not adjacent to *PRDM16*, being ~2 Mb (2,044,815 bp) away from the proximal boundary of *PRDM16*. Case 16 was taken from a publicly available database. Neither *PRDM16* nor *SKI* were deleted and we could not rule out possible mutations in these genes. Other possibilities are that this individual represents a

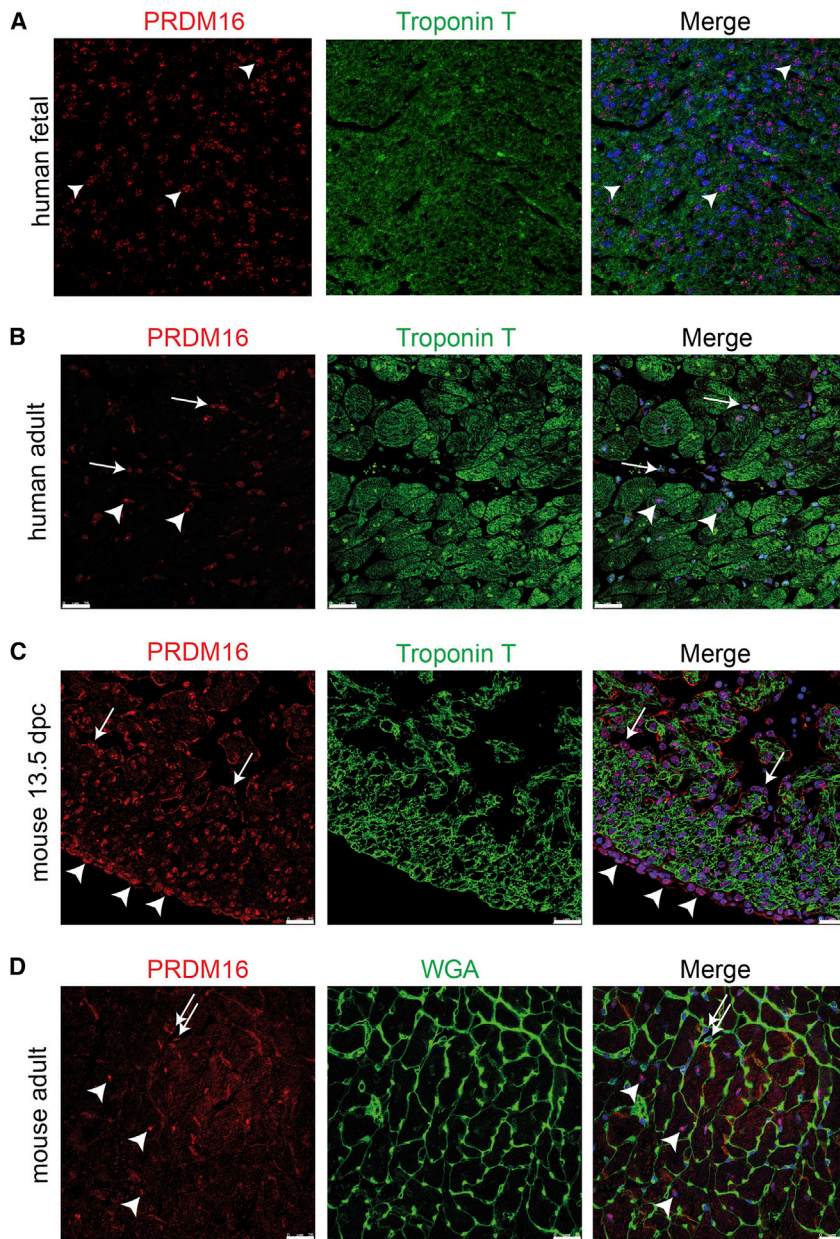


**Figure 3. PRDM16 Localization in the Human and Mouse Heart**

(A and B) Immunofluorescence staining of fetal (A) and adult (B) human left ventricular myocardium showing PRDM16 (in red) in the nuclei (in blue) of both cardiomyocytes (positive for Troponin T, in green, arrowheads) and interstitial cells (arrows).

(C) Within the ventricular myocardium of 13.5 dpc mouse embryos, PRDM16 localization is detectable in cardiomyocytes of the compact and trabeculated layer as well as in epicardial (arrowheads) and endocardial (arrows) cells.

(D) In the adult mouse heart, PRDM16 is located primarily in cardiomyocyte nuclei (identified by WGA membrane staining, in green, see arrowheads), although some non-myocytes show weak PRDM16 staining as well (arrows).

Scale bars represent 25  $\mu$ m.

individuals with 1p36del syndrome that have been published in small and large studies are deleted for this region but do not have any features of LVNC. This observation is in accordance with the observation that incomplete penetrance is a hallmark of the cardiomyopathic phenotypes.<sup>6</sup> Diagnosis is mostly made by echocardiography, and in previously studied cohorts some asymptomatic individuals with 1p36del syndrome with mild LVNC or DCM may not have been recognized.

There appears to be a correlation between the size of the deletion and severity of some clinical features although there is no correlation between the deletion size and number of observed clinical features.<sup>3</sup> Even individuals with deletions <3 Mb can

phenocopy and that another locus than the one on chromosome 1p36 or a nongenetic etiology is responsible for this person's cardiomyopathy.

Notably, the 1p36del syndrome exhibits gender bias, raising the possibilities of a sex-linked modifier or of some form of imprinting.<sup>2</sup> Out of 18 individuals with 1p36del syndrome reported in this study, 16 were females. Further work in zebrafish and extent murine models will help to clarify the mechanistic basis of this effect.

LVNC has recently been classified as a distinct primary cardiomyopathy with a genetic etiology. Mutations in genes encoding sarcomere proteins account for 30% of cases of isolated, nonsyndromic LVNC.<sup>13</sup> LVNC is seen in a number of genetic syndromes, and like DCM has been associated with neuromuscular disorders such as dystrophinopathies and with mitochondrial disease. Many

present with most of the features associated with monosomy 1p36.<sup>32</sup> Individuals with overlapping or even identical regions of deletion demonstrate variable expression of the phenotype.<sup>25</sup> In a case of recurrent monosomy 1p36 observed in siblings secondary to potential germline mosaicism, LVNC was present in both individuals with different severity of the disease.<sup>25</sup> Whereas the one individual showed signs of mild left ventricular dysfunction with DCM that required anticongestive heart failure treatment, the cardiomyopathy of the sibling remained clinically silent. Although these cases share the same underlying molecular etiology of the cardiomyopathic phenotypes, interactions of genetic etiology, background modifier genes, and/or hemodynamic factors most probably contribute to the development of the phenotype.<sup>11</sup>

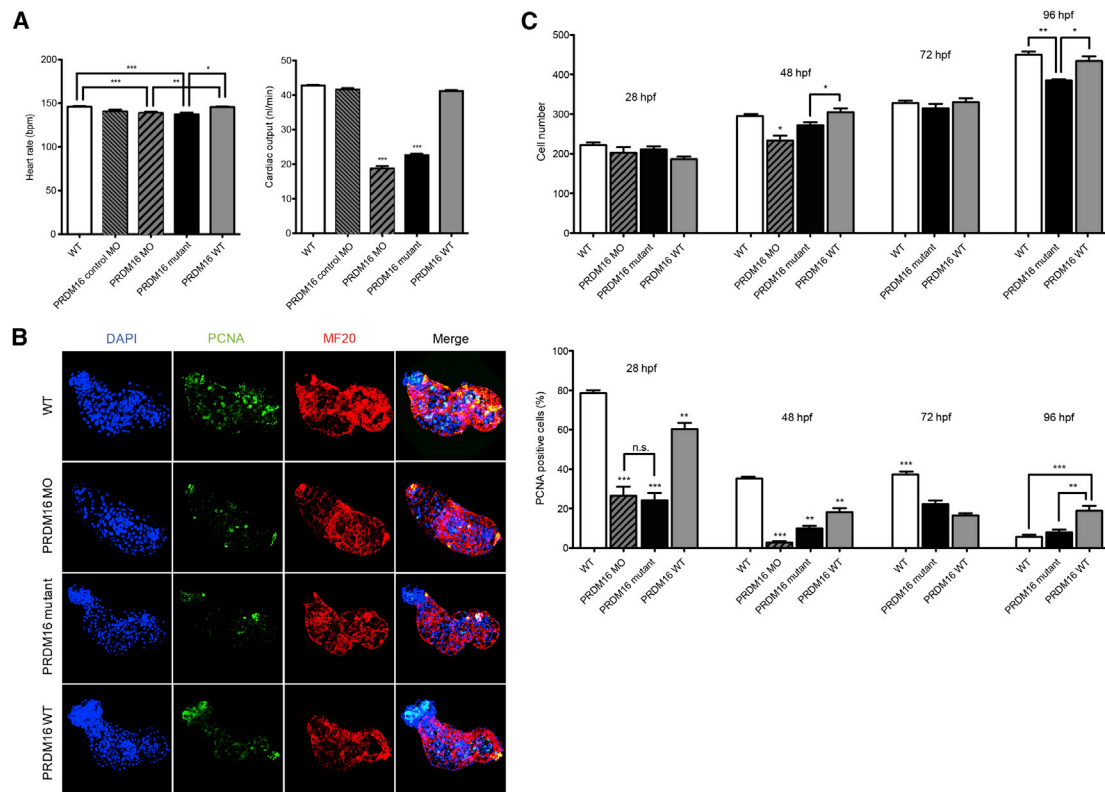


**Figure 4. PRDM16 Knockdown and Human PRDM16 Truncation Mutant in a Zebrafish Model**

(A) There is significantly reduced heart rate and cardiac output in PRDM16 MO and PRDM16 mutant animals compared to WT, MO control, and PRDM16 WT.

(B) In PRDM16 MO and PRDM16 mutant hearts, there is significant reduction in total cell number and rates of cellular proliferation at 48 hpf that is only partially rescued by PRDM16 WT overexpression.

(C) Time-dependent effect of PRDM16 on cell number and proliferation in WT, PRDM16 MO, PRDM16 mutant, and PRDM16 WT embryos. Plotting cell number during cardiac development reveals that both morphant and mutant fish exhibit reduced cell numbers that despite changes in proliferation rates are not fully recovered by 96 hpf. The effects of mutant and wild-type PRDM16 constructs appear to act in opposing directions between 48 or 96 hpf and 72 hpf. The mechanism for this effect is unknown but is not related to changes in the baseline expression of PRDM16.

One-way ANOVA test: \* $p < 0.05$ ; \*\* $p < 0.005$ ; \*\*\* $p < 0.0005$ . The error bars represent the mean  $\pm$  SEM.

PRDM16 acts as a transcription factor with zinc finger DNA-binding domains and positive regulatory (PR), repressor, and acidic domains. PRDM16 regulates leukamogenesis, palatogenesis, neurogenesis, and brown fat development.<sup>26,33–35</sup> Chromosomal translocations resulting in increased expression of isoforms of PRDM16 that lack the PR domain are found recurrently in myelodysplastic syndrome and acute myeloid leukemias.<sup>33</sup> PRDM16 has been shown to direct brown fat determination and differentiation<sup>34</sup> by forming a transcriptional complex with the active form of C/EBP- $\beta$  and acting as a critical complex in the control of the cell fate switch from myoblastic precursors to brown fat cells.<sup>36</sup> PRDM16 has also been described to have a regulatory role in transforming growth factor (TGF)- $\beta$  signaling. A negative effect of PRDM16 on TGF- $\beta$  signaling has been demonstrated in vitro and activated or repressed levels of activity in vivo may disrupt the delicate balance between cell proliferation and differentiation.<sup>26</sup>

Interestingly, PRDM16 has a dominant-positive effect on cardiomyocyte proliferation in zebrafish where either acti-

vated or repressed levels of activity of PRDM16 impair cardiomyocyte proliferation (Figure 4C). This reduction in cell number appears to result from a combination of diminished proliferation and increased apoptosis, possibly through effects mediated via TGF- $\beta$  signaling<sup>26</sup> or interaction with C/EBP- $\beta$ .<sup>36</sup> We noted distinctive effects on subsequent waves of cardiomyocyte proliferation, suggesting that mutant and wild-type PRDM16 are acting in opposite directions, possibly as a result of differential interaction with developmental partners during the serial waves of proliferation in the developing heart.

Perturbation of intercellular coupling can lead to cardiomyopathy and has also been implicated in the regulation of cardiomyocyte differentiation.<sup>37</sup> Specific mutants in cardiac desmosomal genes<sup>38</sup> have suggested abnormalities along the spectrum of differentiation between adipocyte and myocyte<sup>39</sup> and, together with the discovery of PRDM16 mutations, implicate a complex role for electrical or mechanical refinement of a basic transcriptional program in refining myocardial differentiation. PRDM16 has been implicated in the myocyte-adipocyte fate switch



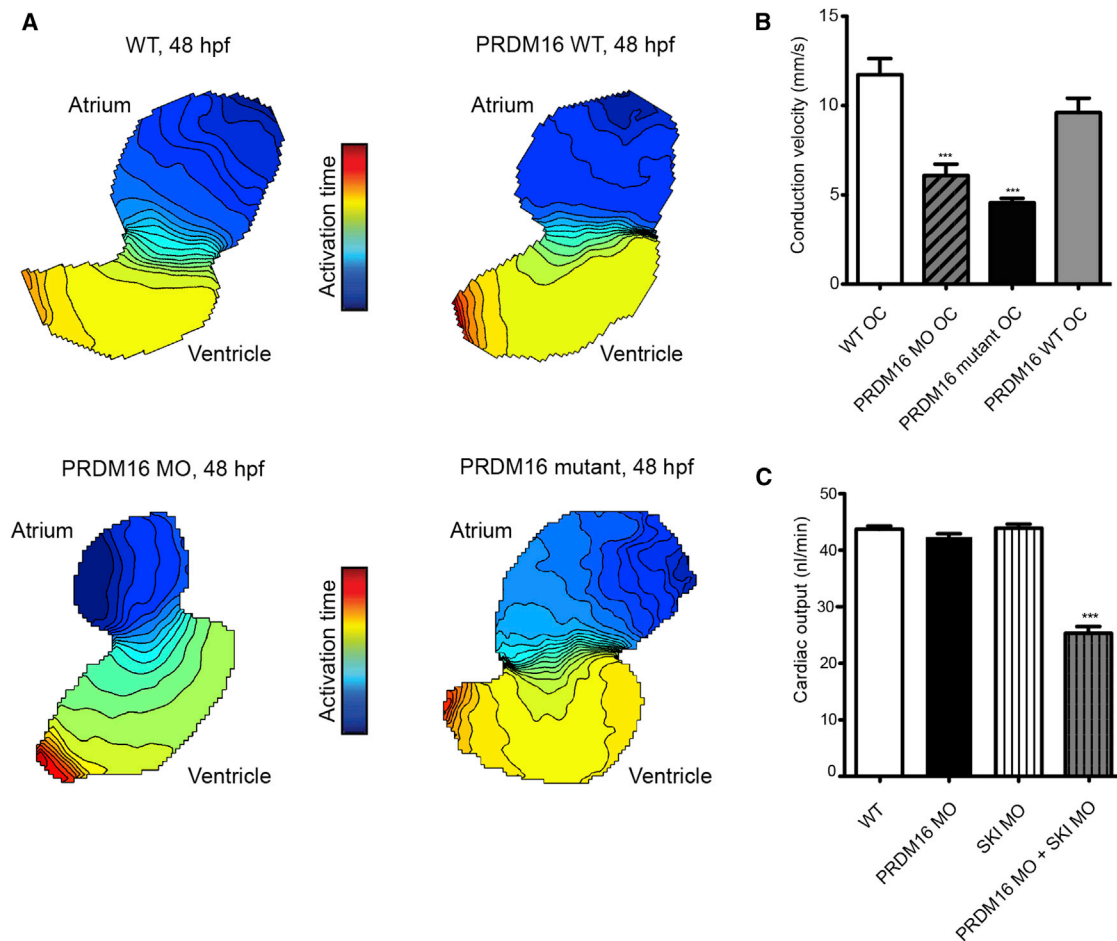


**Figure 5. Cell Coupling in a *PRDM16* Zebrafish Model and Interaction of *PRDM16* with *SKI***

(A) Loss of *PRDM16* leads to partial uncoupling of cardiomyocytes in the zebrafish ventricle. Isochronal maps of wild-type (WT), *PRDM16* WT transgenic, *PRDM16* morphant (MO), and *PRDM16* mutant transgenic hearts. The lines represent the positions of the action potential wavefront at 5 ms intervals. The color scale depicts the timing of electrical activation (blue areas activated before red areas). (B) Mean estimated conduction velocities from the outer curvature of the ventricle (OC) confirm a significant reduction in impulse propagation velocities in morphant and mutant hearts when compared with uninjected controls or wild-type. (C) *PRDM16* and *SKI* double morphant embryos have a more profound effect on cardiac output, suggesting a synergistic genetic interaction.

One-way ANOVA test: \* $p < 0.05$ ; \*\* $p < 0.005$ ; \*\*\* $p < 0.0005$ . The error bars represent the mean  $\pm$  SEM.

in skeletal muscle,<sup>34</sup> and the loss of coupling that characterizes more adipogenic fates may underlie the profound effects we have observed with *PRDM16* knockdown or mutation. The highly orchestrated myocardial coupling evident in the later stages of cardiogenesis may require a critical mass of cardiomyocytes or a critical physiologic stimulus.<sup>40</sup> In addition, the emerging role of epigenetic factors in refining cardiac development, modulating cardiomyocyte differentiation, and establishing definitive cardiac structure and function suggests that there is likely to be complex interplay among these various mechanisms. Interestingly, *PRDM16* helps maintain the integrity of mammalian heterochromatin and the structure of the nuclear lamina.<sup>41</sup> Understanding the reduced stimulus or its transduction failure will provide a unifying framework for the analysis of a wide range of human conditions and animal model phenotypes associated with cardiomyopathy.

In conclusion, we show that mutation of the transcription factor *PRDM16* is an important cause of cardiomyopathy in individuals with the chromosome 1p36 deletion syndrome as well as in nonsyndromic forms of LVNC and DCM. Our functional studies implicate impaired proliferative capacity during cardiogenesis as a primary mechanism of these *PRDM16*-related cardiomyopathies and suggest a pathway in human heart failure that may be amenable to therapeutic intervention.

#### Supplemental Data

Supplemental Data include five figures and two tables and can be found with this article online at <http://www.cell.com/AJHG/>.

#### Acknowledgments

This study makes use of data generated by the DECIPHER Consortium. A full list of centers that contributed to the generation

of the data is available from <http://decipher.sanger.ac.uk> and via email from [decipher@sanger.ac.uk](mailto:decipher@sanger.ac.uk) and funding of the project was provided by the Wellcome Trust. We are pleased to cite the database Ecaruca for cytogenetic information. We are grateful to L. Thierfelder, S. Bähring, and F.C. Luft for infrastructural support. This study was supported by the Competence Network for Congenital Heart Defects, Germany, funded by the Federal Ministry of Education and Research (BMBF), FKZ01GI0601, the DZHK (German Centre for Cardiovascular Research) as well as support to C.A.M. from the Harvard Stem Cell Institute and the Leducq Foundation. S.A.C. is supported by the Fondation Leducq. S.A.C. and P.J.B. are supported by the National Institute for Health Research Cardiovascular BRU at the Brompton and Harefield & Harefield NHS Foundation Trust and Imperial College London and P.J.B. by Heart Research U.K. A.-K.A. was supported by a personal grant from the Deutsche Herzstiftung.

Received: April 10, 2013  
 Revised: May 5, 2013  
 Accepted: May 20, 2013  
 Published: June 13, 2013

## Web Resources

The URLs for data presented herein are as follows:

1000 Genomes, <http://browser.1000genomes.org>  
 dbSNP, <http://www.ncbi.nlm.nih.gov/projects/SNP/>  
 DECIPHER, <https://decipher.sanger.ac.uk/>  
 ECARUCA database, <http://umcecaruca01.extern.umcn.nl:8080/ecaruca/ecaruca.jsp>  
 Genoglyphix, <http://www.signaturegenomics.com/genoglyphix.html>  
 NHLBI Exome Sequencing Project (ESP) Exome Variant Server, <http://evs.gs.washington.edu/EVS/>  
 NCBI, <http://www.ncbi.nlm.nih.gov/>  
 Online Mendelian Inheritance in Man (OMIM), <http://www.omim.org/>  
 PolyPhen-2, <http://www.genetics.bwh.harvard.edu/pph2/>  
 RefSeq, <http://www.ncbi.nlm.nih.gov/RefSeq>  
 SIFT, <http://sift.bii.a-star.edu.sg/>  
 UniProt, <http://www.uniprot.org/>  
 UCSC Genome Browser, <http://genome.ucsc.edu>

## References

- Shaffer, L.G., and Lupski, J.R. (2000). Molecular mechanisms for constitutional chromosomal rearrangements in humans. *Annu. Rev. Genet.* *34*, 297–329.
- Shapira, S.K., McCaskill, C., Northrup, H., Spikes, A.S., Elder, F.E., Sutton, V.R., Korenberg, J.R., Greenberg, F., and Shaffer, L.G. (1997). Chromosome 1p36 deletions: the clinical phenotype and molecular characterization of a common newly delineated syndrome. *Am. J. Hum. Genet.* *61*, 642–650.
- Heilstedt, H.A., Ballif, B.C., Howard, L.A., Lewis, R.A., Stal, S., Kashork, C.D., Bacino, C.A., Shapira, S.K., and Shaffer, L.G. (2003). Physical map of 1p36, placement of breakpoints in monosomy 1p36, and clinical characterization of the syndrome. *Am. J. Hum. Genet.* *72*, 1200–1212.
- Battaglia, A., Hoyne, H.E., Dallapiccola, B., Zackai, E., Hudgins, L., McDonald-McGinn, D., Bahi-Buisson, N., Romano, C., Williams, C.A., Brailey, L.L., et al. (2008). Further delineation of deletion 1p36 syndrome in 60 patients: a recognizable phenotype and common cause of developmental delay and mental retardation. *Pediatrics* *121*, 404–410.
- Jenni, R., Oechslin, E., Schneider, J., Attenhofer Jost, C., and Kaufmann, P.A. (2001). Echocardiographic and pathoanatomical characteristics of isolated left ventricular non-compaction: a step towards classification as a distinct cardiomyopathy. *Heart* *86*, 666–671.
- McNally, E.M., Golbus, J.R., and Puckelwartz, M.J. (2013). Genetic mutations and mechanisms in dilated cardiomyopathy. *J. Clin. Invest.* *123*, 19–26.
- Klopocki, E., Schulze, H., Strauss, G., Ott, C.E., Hall, J., Trotier, F., Fleischhauer, S., Greenhalgh, L., Newbury-Ecob, R.A., Neumann, L.M., et al. (2007). Complex inheritance pattern resembling autosomal recessive inheritance involving a microdeletion in thrombocytopenia-absent radius syndrome. *Am. J. Hum. Genet.* *80*, 232–240.
- Caliebe, A., Kroes, H.Y., van der Smagt, J.J., Martin-Subero, J.I., Tönnies, H., van 't Slot, R., Nievelein, R.A., Muhle, H., Stephani, U., Alfke, K., et al. (2010). Four patients with speech delay, seizures and variable corpus callosum thickness sharing a 0.440 Mb deletion in region 1q44 containing the HNRPU gene. *Eur. J. Med. Genet.* *53*, 179–185.
- Firth, H.V., Richards, S.M., Bevan, A.P., Clayton, S., Corpas, M., Rajan, D., Van Vooren, S., Moreau, Y., Pettett, R.M., and Carter, N.P. (2009). DECIPHER: Database of Chromosomal Imbalance and Phenotype in Humans Using Ensembl Resources. *Am. J. Hum. Genet.* *84*, 524–533.
- Feenstra, I., Fang, J., Koolen, D.A., Siezen, A., Evans, C., Winter, R.M., Lees, M.M., Riegel, M., de Vries, B.B., Van Ravenswaaij, C.M., and Schinzel, A. (2006). European Cytogeneticists Association Register of Unbalanced Chromosome Aberrations (ECARUCA); an online database for rare chromosome abnormalities. *Eur. J. Med. Genet.* *49*, 279–291.
- Klaassen, S., Probst, S., Oechslin, E., Gerull, B., Krings, G., Schuler, P., Greutmann, M., Hürlimann, D., Yegitbasi, M., Pons, L., et al. (2008). Mutations in sarcomere protein genes in left ventricular noncompaction. *Circulation* *117*, 2893–2901.
- Mestroni, L., Maisch, B., McKenna, W.J., Schwartz, K., Charon, P., Rocco, C., Tesson, F., Richter, A., Wilke, A., and Komajda, M.; Collaborative Research Group of the European Human and Capital Mobility Project on Familial Dilated Cardiomyopathy. (1999). Guidelines for the study of familial dilated cardiomyopathies. *Eur. Heart J.* *20*, 93–102.
- Probst, S., Oechslin, E., Schuler, P., Greutmann, M., Boyé, P., Knirsch, W., Berger, F., Thierfelder, L., Jenni, R., and Klaassen, S. (2011). Sarcomere gene mutations in isolated left ventricular noncompaction cardiomyopathy do not predict clinical phenotype. *Circ. Cardiovasc. Genet.* *4*, 367–374.
- Trapnell, C., Pachter, L., and Salzberg, S.L. (2009). TopHat: discovering splice junctions with RNA-Seq. *Bioinformatics* *25*, 1105–1111.
- Flicek, P., Amode, M.R., Barrell, D., Beal, K., Brent, S., Carvalho-Silva, D., Clapham, P., Coates, G., Fairley, S., Fitzgerald, S., et al. (2012). Ensembl 2012. *Nucleic Acids Res.* *40*(Database issue), D84–D90.
- Li, H., Handsaker, B., Wysoker, A., Fennell, T., Ruan, J., Homer, N., Marth, G., Abecasis, G., and Durbin, R.; 1000 Genome Project Data Processing Subgroup. (2009). The Sequence

- Alignment/Map format and SAMtools. *Bioinformatics* 25, 2078–2079.
17. Milan, D.J., Giokas, A.C., Serluca, F.C., Peterson, R.T., and MacRae, C.A. (2006). Notch1b and neuregulin are required for specification of central cardiac conduction tissue. *Development* 133, 1125–1132.
  18. Werdich, A.A., Brzezinski, A., Jeyaraj, D., Khaled Sabeh, M., Ficker, E., Wan, X., McDermott, B.M., Jr., Macrae, C.A., and Rosenbaum, D.S. (2012). The zebrafish as a novel animal model to study the molecular mechanisms of mechano-electrical feedback in the heart. *Prog. Biophys. Mol. Biol.* 110, 154–165.
  19. van Ham, T.J., Mapes, J., Kokel, D., and Peterson, R.T. (2010). Live imaging of apoptotic cells in zebrafish. *FASEB J.* 24, 4336–4342.
  20. Colmenares, C., Heilstedt, H.A., Shaffer, L.G., Schwartz, S., Berk, M., Murray, J.C., and Stavnezer, E. (2002). Loss of the SKI proto-oncogene in individuals affected with 1p36 deletion syndrome is predicted by strain-dependent defects in Ski-/- mice. *Nat. Genet.* 30, 106–109.
  21. Giannikou, K., Fryssira, H., Oikonomakis, V., Syrmou, A., Kosma, K., Tzetis, M., Kitsiou-Tzeli, S., and Kanavakis, E. (2012). Further delineation of novel 1p36 rearrangements by array-CGH analysis: narrowing the breakpoints and clarifying the “extended” phenotype. *Gene* 506, 360–368.
  22. Rosenfeld, J.A., Crolla, J.A., Tomkins, S., Bader, P., Morrow, B., Gorski, J., Troxell, R., Forster-Gibson, C., Cilliers, D., Hislop, R.G., et al. (2010). Refinement of causative genes in monosomy 1p36 through clinical and molecular cytogenetic characterization of small interstitial deletions. *Am. J. Med. Genet. A.* 152A, 1951–1959.
  23. Heilstedt, H.A., Burgess, D.L., Anderson, A.E., Chedrawi, A., Tharp, B., Lee, O., Kashork, C.D., Starkey, D.E., Wu, Y.Q., Noebels, J.L., et al. (2001). Loss of the potassium channel beta-subunit gene, KCNAB2, is associated with epilepsy in patients with 1p36 deletion syndrome. *Epilepsia* 42, 1103–1111.
  24. Gajecka, M., Yu, W., Ballif, B.C., Glotzbach, C.D., Bailey, K.A., Shaw, C.A., Kashork, C.D., Heilstedt, H.A., Ansel, D.A., Theisen, A., et al. (2005). Delineation of mechanisms and regions of dosage imbalance in complex rearrangements of 1p36 leads to a putative gene for regulation of cranial suture closure. *Eur. J. Hum. Genet.* 13, 139–149.
  25. Gajecka, M., Saitta, S.C., Gentles, A.J., Campbell, L., Ciprero, K., Geiger, E., Catherwood, A., Rosenfeld, J.A., Shaikh, T., and Shaffer, L.G. (2010). Recurrent interstitial 1p36 deletions: evidence for germline mosaicism and complex rearrangement breakpoints. *Am. J. Med. Genet. A.* 152A, 3074–3083.
  26. Bjork, B.C., Turbe-Doan, A., Prysak, M., Herron, B.J., and Beier, D.R. (2010). Prdm16 is required for normal palatogenesis in mice. *Hum. Mol. Genet.* 19, 774–789.
  27. Doyle, A.J., Doyle, J.J., Bessling, S.L., Maragh, S., Lindsay, M.E., Schepers, D., Gillis, E., Mortier, G., Homfray, T., Sauls, K., et al. (2012). Mutations in the TGF- $\beta$  repressor SKI cause Shprintzen-Goldberg syndrome with aortic aneurysm. *Nat. Genet.* 44, 1249–1254.
  28. Carmignac, V., Thevenon, J., Adès, L., Callewaert, B., Julia, S., Thauvin-Robinet, C., Gueneau, L., Courcet, J.B., Lopez, E., Holman, K., et al. (2012). In-frame mutations in exon 1 of SKI cause dominant Shprintzen-Goldberg syndrome. *Am. J. Hum. Genet.* 91, 950–957.
  29. Bulger, M., and Groudine, M. (2011). Functional and mechanistic diversity of distal transcription enhancers. *Cell* 144, 327–339.
  30. Redon, R., Rio, M., Gregory, S.G., Cooper, R.A., Fiegler, H., Sanlaville, D., Banerjee, R., Scott, C., Carr, P., Langford, C., et al. (2005). Tiling path resolution mapping of constitutional 1p36 deletions by array-CGH: contiguous gene deletion or “deletion with positional effect” syndrome? *J. Med. Genet.* 42, 166–171.
  31. Kleinjan, D.J., and van Heyningen, V. (1998). Position effect in human genetic disease. *Hum. Mol. Genet.* 7, 1611–1618.
  32. Gajecka, M., Mackay, K.L., and Shaffer, L.G. (2007). Monosomy 1p36 deletion syndrome. *Am. J. Med. Genet. C. Semin. Med. Genet.* 145C, 346–356.
  33. Mochizuki, N., Shimizu, S., Nagasawa, T., Tanaka, H., Taniwaki, M., Yokota, J., and Morishita, K. (2000). A novel gene, MEL1, mapped to 1p36.3 is highly homologous to the MDS1/EVI1 gene and is transcriptionally activated in t(1;3)(p36;q21)-positive leukemia cells. *Blood* 96, 3209–3214.
  34. Seale, P., Bjork, B., Yang, W., Kajimura, S., Chin, S., Kuang, S., Scimè, A., Devarakonda, S., Conroe, H.M., Erdjument-Bromage, H., et al. (2008). PRDM16 controls a brown fat/skeletal muscle switch. *Nature* 454, 961–967.
  35. Kinameri, E., Inoue, T., Aruga, J., Imayoshi, I., Kageyama, R., Shimogori, T., and Moore, A.W. (2008). Prdm proto-oncogene transcription factor family expression and interaction with the Notch-Hes pathway in mouse neurogenesis. *PLoS ONE* 3, e3859.
  36. Kajimura, S., Seale, P., Kubota, K., Lunsford, E., Frangioni, J.V., Gygi, S.P., and Spiegelman, B.M. (2009). Initiation of myoblast to brown fat switch by a PRDM16-C/EBP-beta transcriptional complex. *Nature* 460, 1154–1158.
  37. Panáková, D., Werdich, A.A., and Macrae, C.A. (2010). Wnt11 patterns a myocardial electrical gradient through regulation of the L-type Ca(2+) channel. *Nature* 466, 874–878.
  38. Gerull, B., Heuser, A., Wichter, T., Paul, M., Basson, C.T., McDermott, D.A., Lerman, B.B., Markowitz, S.M., Ellinor, P.T., MacRae, C.A., et al. (2004). Mutations in the desmosomal protein plakophilin-2 are common in arrhythmogenic right ventricular cardiomyopathy. *Nat. Genet.* 36, 1162–1164.
  39. Lombardi, R., da Graca Cabreira-Hansen, M., Bell, A., Fromm, R.R., Willerson, J.T., and Marian, A.J. (2011). Nuclear plakoglobin is essential for differentiation of cardiac progenitor cells to adipocytes in arrhythmogenic right ventricular cardiomyopathy. *Circ. Res.* 109, 1342–1353.
  40. Boström, P., Mann, N., Wu, J., Quintero, P.A., Plovie, E.R., Panáková, D., Gupta, R.K., Xiao, C., MacRae, C.A., Rosenzweig, A., and Spiegelman, B.M. (2010). C/EBP $\beta$  controls exercise-induced cardiac growth and protects against pathological cardiac remodeling. *Cell* 143, 1072–1083.
  41. Pinheiro, I., Margueron, R., Shukeir, N., Eisold, M., Fritsch, C., Richter, F.M., Mittler, G., Genoud, C., Goyama, S., Kurokawa, M., et al. (2012). Prdm3 and Prdm16 are H3K9me1 methyltransferases required for mammalian heterochromatin integrity. *Cell* 150, 948–960.